

Higgs-Higgsino-Gaugino Induced Two Loop Electric Dipole Moments

Yingchuan Li,^{1,*} Stefano Profumo,^{2,†} and Michael Ramsey-Musolf^{1,‡}

¹*Department of Physics, University of Wisconsin, Madison, Wisconsin 53705*

²*Department of Physics and Santa Cruz Institute for Particle Physics,
University of California, 1156 High St., Santa Cruz, CA 95064, USA*

(Dated: April 23, 2019)

Abstract

We compute the complete set of Higgs-mediated chargino-neutralino two-loop contributions to the electric dipole moments (EDMs) of the electron and neutron in the minimal supersymmetric standard model (MSSM). We study the dependence of these contributions on the parameters that govern CP-violation in the MSSM gauge-gaugino-Higgs-Higgsino sector. We find that contributions mediated by the exchange of $W^\pm H^\mp$ and ZA^0 pairs, where H^\pm and A^0 are the charged and CP-odd Higgs scalars, respectively, are comparable to those mediated by the exchange of neutral gauge bosons and CP-even Higgs scalars. We also find that strong cancellations between the various contributions can occur in various regions of the MSSM parameter space, implying the possibility of two-loop EDMs that could evade future experimental EDM searches. We also emphasize that the result of this complete set of diagrams is essential for the full quantitative study of a number of phenomenologies and their correlations, such as electric dipole moment, and electroweak baryogenesis. In particular, we point out that the cancellations we find are unlikely to occur in parameter space regions favored by the requirement of successful MSSM electroweak baryogenesis.

*Electronic address: yli@physics.umd.edu

†Electronic address: profumo@scipp.ucsc.edu

‡Electronic address: mjrm@physics.wisc.edu

I. INTRODUCTION

The search for CP-violation (CPV) beyond that of the Standard Model (SM) lies at the forefront of nuclear and particle physics. Perhaps the most powerful probes for new CPV are searches for permanent electric dipole moments (EDMs) of the electron, neutron, and neutral atoms. Null results obtained from these searches have placed stringent constraints on CPV in the strong sector of the SM, while present and expected future sensitivities lie several orders of magnitude away from expectations based on CPV associated with the phase of the Cabibbo-Kobayashi-Maskawa (CKM) matrix. Various scenarios for CPV connected to new physics at or above the electroweak scale naturally imply the existence of non-vanishing EDMs that could be observed in future experiments. Thus, a comprehensive program of EDM searches could uncover either CPV associated with the “ θ -term” of the QCD Lagrangian, new electroweak scale physics, or both. Each possibility has potentially significant consequences for cosmology. The Peccei-Quinn mechanism proposed to explain the vanishingly small value of $\bar{\theta}$ implies the existence of an axion that could account for the cold dark matter (CDM), while new electroweak scale CPV could help in explaining the observed abundance of baryonic matter through the mechanism of electroweak baryogenesis (EWB).

Among the most theoretically attractive possibilities for new physics is supersymmetry (SUSY). SUSY provides an appealing solution to the naturalness problem of the SM. However, SUSY has to be softly broken to be consistent with experimental observations. In order to solve the naturalness problem, the SUSY breaking scale should be not much higher than a few TeV. While the exact mechanism of soft SUSY breaking is not yet known, its effect is encoded into the soft terms in the low-energy realization of this scenario. In the minimal supersymmetric standard model (MSSM), the presence of soft terms implies the existence of 40 additional CPV phases beyond the single phase of the CKM matrix in the SM. As there exists no known *a priori* reason for these phases to be suppressed, one expects rather sizable EDMs to be generated by one-loop graphs when supersymmetric particle masses are below ~ 1 TeV.

However, the current experiment bounds on electron, neutron EDM, and ^{199}Hg atom are already tight: $|d_e| < 1.6 \times 10^{-27} e \text{ cm}$ (90% C.L.) [1], $|d_n| < 2.9 \times 10^{-27} e \text{ cm}$ (90% C.L.) [2], and $|d_A(^{199}\text{Hg})| < 2.1 \times 10^{-27} e \text{ cm}$ (95% C.L.) [3] (For recent reviews of EDM searches and their implications for SUSY, see, *e.g.* Refs. [4, 5]). These results imply CPV phases of order 10^{-3} or smaller, leading to the so-called “SUSY CP problem”. Its resolution, as well as that of the related “SUSY flavor problem”, requires some other mechanism for suppressing one-loop EDMs (and one-loop flavor changing neutral currents). One possibility is to take the masses of the first and second generation sfermions to be of order 10 TeV [6]. In such circumstances, the one-loop contributions to EDMs are highly suppressed, and the two-loop contributions to EDM, with CP violations from either chargino-neutralino sector or the third generation of squarks, may give competitive and even dominate contributions to EDMs of the electron and neutron¹.

Previous work has considered a subset of these two-loop contributions, including those involving third generation squarks [7, 8] and charginos [9, 10, 11, 12] whose CPV interactions with the gauge-Higgs sector of the MSSM induce an EDM (or chromo-EDM) of

¹ The EDMs of diamagnetic atoms such as ^{199}Hg will be suppressed in this limit, as they are generated primarily by the one-loop chromo-EDM operators.

an elementary, first generation SM fermion. In particular, implications for CP violation at high-energy colliders and dominant higher-loop contributions were discussed in detail in Ref. [10]. The CP violation from chargino (χ^+)-neutralino (χ^0) sector can be propagated to the SM fermion through purely gauge boson exchanges. In this case, it has been shown that no CP violation can be propagated through $\gamma\gamma$, γZ , and ZZ exchanges [11], leaving the WW exchange as the only possibility. This contribution was recently calculated in Ref. [11, 12]. CP violation can also be propagated through the exchange of gauge and Higgs boson pairs, including γh^0 , γH^0 , Zh^0 , ZH^0 , γA^0 , ZA^0 , and WH^\pm . Here, h^0 and H^0 denote the neutral, CP-even Higgs scalars of the MSSM, with h^0 being the lightest, “SM-like” scalar; A^0 is the neutral CP-odd scalar; and H^\pm denotes the charged scalars. The contributions due to γh^0 , γH^0 , Zh^0 , ZH^0 , and γA^0 exchanges have been studied [9, 10, 11, 12].

In what follows, we compute the remaining two-loop contributions that survive in the limit of large sfermion masses: Barr-Zee [13] type amplitudes wherein chargino-neutralino loops communicate CPV to the fermion via the exchange of a ZA^0 or WH^\pm pair. We also compute the γh^0 , γH^0 , Zh^0 , ZH^0 , and γA^0 contributions, and compare our results with the previous computations reported in Refs. [9, 10, 11, 12]. We find agreement with all the previous results. We find that, in general, the new contributions can be comparable in magnitude to those previously computed. The ZA^0 contribution is accidentally suppressed in the case of the electron EDM by the $1 - 4\sin^2\theta_W$ factor, but it is important for the neutron EDM. Unlike the case of two-loop diagrams with CP violation from squarks, where it has been noted that the γh^0 and γA^0 contributions dominate [7, 8], we find – after completing a numerical study of the analytic results – that the WH^\pm contribution is the dominant one for electron EDM, and both the Z plus h^0 , A^0 and the WH^\pm contributions are the dominant ones for the neutron EDM, proving that the inclusion of these contributions is indispensable. Moreover, we also find that strong cancellations can occur between various two loop contributions in some parts of the MSSM parameter space. It is thus possible that both the magnitude of both one- and two-loop EDMs may fall below the reach of future EDM searches, even allowing for $\mathcal{O}(1)$ CPV phases.

Apart from the implications for EDM phenomenology, our results also have interesting consequences for the viability of supersymmetric EWB. Indeed, part of our original motivation for computing the loops containing the A^0 and H^\pm is that the masses of these scalars affects the dynamics of supersymmetric EWB. In particular, during a first order electroweak phase transition that proceeds via bubble nucleation, the rate at which the neutral Higgs vacuum expectation values (vevs) change across the bubble walls depends on m_{A^0} (which also sets the scale for m_{H^\pm}). Since the CP-violating asymmetries needed for baryon number production are generated during the phase transition by scattering from these vevs, knowledge of the bubble wall profiles and their dependence on the other MSSM parameters is essential for determining the viability of supersymmetric EWB. In general, SUSY EWB is enhanced for relatively light m_{A^0} – a region in which the corresponding ZA^0 , γA^0 , and WH^\pm EDM contributions are also enhanced. In our numerical study of the two-loop EDMs, we investigate the corresponding m_{A^0} -dependence with an eye to these implications for EWB. In doing so, we show that the parameter region in which cancellations are likely to suppress the two-loop EDMs, does not generally coincide with the regions favored by EWB in the MSSM.

Our discussion of these points is organized in the remainder of the paper as follows. In Section II we provide details of our two-loop computation and the analytic expressions for the results. Section III gives our numerical analysis. We summarize our results in Section IV,

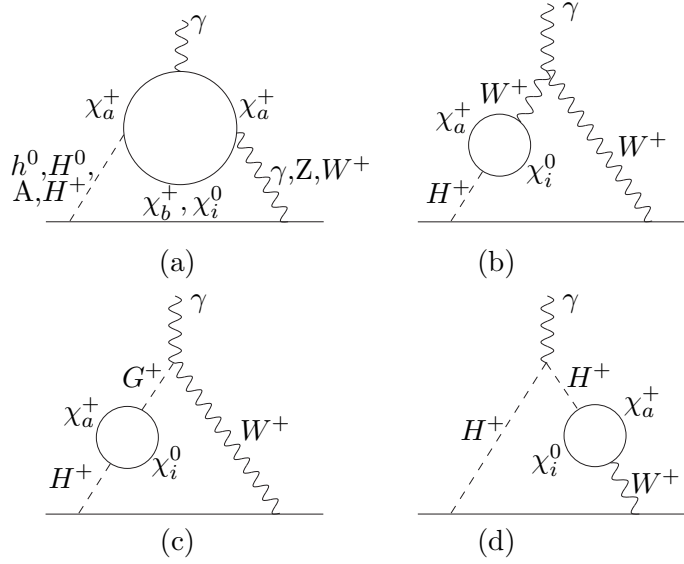


FIG. 1: All the two-loop diagrams with chargino-neutralino loop mediated by Higgs bosons. (Mirror graphs are not displayed.)

while additional technical details are provided in the Appendix. We note that, during the course of completing our study, a parallel computation of the two-loop EDMs in SUSY using an effective field theory approach also appeared [14]. We comment on the similarities and differences we find with that analysis.

II. TWO LOOP EDMs: HIGGS-GAUGE MEDIATED $\chi^+-\chi^0$ CONTRIBUTIONS

Representative diagrams from the various topologies we consider are shown in Fig. 1. For simplicity we have not shown the different crossed graphs or those in which scalar and vector boson lines are interchanged. In addition, diagrams involving a photon insertion on the SM fermion line are also not shown, as these contributions vanish. Of the remaining, non-vanishing diagrams, the contributions with neutral Higgs boson exchange, namely, γh^0 , γH^0 , $Z h^0$, $Z H^0$, and γA^0 , $Z A^0$, only involve diagram (a), while the contributions with charged Higgs boson exchange $W^\mp H^\pm$ involve all the diagrams (a,b,c,d). To simplify the computation of the latter, we follow Ref. [8] and use the nonlinear R_ξ gauge [15]. The corresponding gauge-fixing term in the Lagrangian is obtained by replacing the ordinary derivative that appears in the R_ξ gauge

$$\mathcal{L}_{\text{g.f.}}^{R_\xi} = -\frac{1}{2\xi} |\partial_\mu W_\mu^+ - i\xi M_W \phi^+|^2, \quad (1)$$

with the $U(1)_{\text{EM}}$ covariant derivative $D_\mu = \partial_\mu - ieA_\mu$ in nonlinear R_ξ gauge

$$\mathcal{L}_{\text{g.f.}}^{\text{nonlinear } R_\xi} = -\frac{1}{2\xi} |D_\mu W_\mu^+ - i\xi M_W \phi^+|^2. \quad (2)$$

Thus, just as the R_ξ gauge is designed to eliminate mixing between the would-be Goldstone boson G^\pm and the W^\pm implied by the Higgs kinetic term $(D_\mu \phi)^\dagger (D^\mu \phi)$, the nonlinear R_ξ

gauge is constructed in such a way that the coupling $G^\pm W^\mp \gamma$ arising from the same kinetic term is also canceled. As a result, the $W^+ W^- \gamma$ vertex is modified from its standard form in the conventional renormalizable gauges.

A direct – and simplifying – consequence of employing the nonlinear R_ξ gauge is that the contribution from diagram (c) vanishes due to the absence of the $G^\pm W^\mp \gamma$ coupling. Moreover, an additional simplification can be obtained when carrying out the computation in the Landau gauge ($\xi \rightarrow 0$). In doing so, one must take care to first compute the $\xi \neq 0$ contributions to the $W^+ W^- \gamma$ vertex and W -boson propagators in Fig. 1(b) and carry out the appropriate contractions that appear in the one-loop amplitude before taking the $\xi \rightarrow 0$ limit, since the additional contribution to the $W^+ W^- \gamma$ vertex arising in the nonlinear R_ξ gauge is proportional to $1/\xi$. The resulting simplification is that the amplitude from Fig. 1(d) vanishes as well. This is because the chargino-neutralino loop in (d) is proportional to the four momentum of W boson, while the propagator of W is transverse in Landau gauge.

In carrying out the calculation, we first compute out the one-loop sub-graphs corresponding to the amplitude for $\gamma(q, \mu) \rightarrow h(q - \ell) + g(\ell, \nu)$, where h stands for one of Higgs bosons (h^0, H^0, A^0, H^\pm) having momentum $q - \ell$; g denotes one of gauge bosons (γ, Z, W) having momentum ℓ ; and μ and ν denote the vector indices associated with the external photon and g , respectively. Gauge invariance implies that the amplitude involves a linear combination of the (pseudo) tensors

$$\begin{aligned} P^{\mu\nu} &= \epsilon^{\mu\nu\alpha\beta} q_\alpha \ell_\beta \\ T^{\mu\nu} &= \ell^\mu q^\nu - g^{\mu\nu} \ell \cdot q \quad . \end{aligned} \quad (3)$$

For the full two-loop graphs involving the exchange of neutral bosons, only $P^{\mu\nu}$ contributes in the case of CP-even Higgs exchange, while only $T^{\mu\nu}$ contributes for the graphs involving the CP-odd Higgs. Both $P^{\mu\nu}$ and $T^{\mu\nu}$ contribute to the two-loop WH^\pm amplitude. For our particular gauge choice, we find that $P^{\mu\nu}$ arises from diagram Fig. 1(a) alone, while for $W^\mp H^\pm$ exchange, $T^{\mu\nu}$ requires the sum of both Fig. 1(a) and (b) [graph (b) only generates a $\ell \cdot q g^{\mu\nu}$ structure]. We will use these features to explain the origin of the overall, relative signs between the various contributions below.

In obtaining our final results for the two-loop contributions, we use the Feynman rules and conventions given in Ref. [16]². We have attempted to express our results in a manner that makes easy to directly compare with the earlier work of Refs. [9, 10, 11, 12]. We find

$$d_f^{ZS} = \frac{e Q_f \alpha^2 c_f^S}{8\sqrt{2}\pi^2 s_W^2} \frac{m_f}{M_W m_S^2} \sum_{a=1}^2 \text{Im}(D_{S,aa}^R) M_{\chi_a^+} \int_0^1 dx \frac{1}{x(1-x)} j(0, \frac{r_{aS}}{x(1-x)}), \quad (4)$$

$$\begin{aligned} d_f^{ZS} &= \frac{e\alpha^2 (T_{3fL} - 2s_W^2 Q_f) c_f^S}{16\sqrt{2}\pi^2 c_W^2 s_W^4} \frac{m_f}{M_W m_S^2} \\ &\times \sum_{a,b=1}^2 \text{Im}(G_{ab}^R D_{S,ba}^R - G_{ab}^L D_{S,ba}^L) M_{\chi_b^+} \int_0^1 dx \frac{1}{x} j(r_{ZS}, \frac{x r_{aS} + (1-x) r_{bS}}{x(1-x)}), \quad (5) \end{aligned}$$

² However, our convention for the Higgs scalar mixing angle α differs from that of Ref. [16]. To facilitate comparison with results appearing in the literature, we adopt the convention of Ref. [12].

$$d_f^{A^0} = \frac{eQ_f\alpha^2 c_f^{A^0}}{8\sqrt{2}\pi^2 s_W^2} \frac{m_f}{M_W m_{A^0}^2} \sum_{a=1}^2 \text{Im} E_{aa}^R M_{\chi_a^+} \int_0^1 dx \frac{1-2x+2x^2}{x(1-x)} j(0, \frac{r_{aA^0}}{x(1-x)}), \quad (6)$$

$$d_f^{ZA^0} = \frac{e\alpha^2 (T_{3fL} - 2s_W^2 Q_f) c_f^{A^0}}{16\sqrt{2}\pi^2 c_W^2 s_W^4} \frac{m_f}{M_W m_{A^0}^2} \times \sum_{a,b=1}^2 \text{Im}(G_{ab}^R E_{ba}^R + G_{ab}^L E_{ba}^L) M_{\chi_b^+} \int_0^1 dx \frac{1-x}{x} j(r_{ZA^0}, \frac{x r_{aA^0} + (1-x) r_{bA^0}}{x(1-x)}), \quad (7)$$

$$d_f^{WH^\pm} = -\frac{e\alpha^2 c_f^{H^\pm}}{32\pi^2 s_W^4 c_W} \frac{m_f}{M_W m_{H^\pm}^2} \sum_{a=1}^2 \sum_{i=1}^4 \int_0^1 dx \frac{1}{1-x} j(r_{WH^\pm}, \frac{r_{aH^\pm}}{1-x} + \frac{r_{iH^\pm}}{x}) \left[(\text{Im}(M_{ai}^L N_{ai}^{L*} + M_{ai}^R N_{ai}^{R*}) M_{\chi_a^+} x^2 + \text{Im}(M_{ai}^R N_{ai}^{L*} + M_{ai}^L N_{ai}^{R*}) M_{\chi_i^0} (1-x)^2) \right. \\ \left. + (\text{Im}(M_{ai}^L N_{ai}^{L*} - M_{ai}^R N_{ai}^{R*}) M_{\chi_a^+} x + \text{Im}(M_{ai}^R N_{ai}^{L*} - M_{ai}^L N_{ai}^{R*}) M_{\chi_i^0} (1-x)) \right] \quad (8)$$

Here, $s_W = \sin\theta_W$ and $c_W = \cos\theta_W$. The S in Eq. (3) and (4) denotes h^0 and H^0 . The symbol $f = u, d, e$ represents the up quark, down quark, and electron, respectively; Q_f and m_f are the electric charge and mass, respectively, of fermion f , and T_{3fL} is the third component of the weak isospin of its left-handed component; finally, $j(r, r')$ is the loop function defined in Ref. [11] and given in the Appendix.

The mass ratios in loop functions are $r_{Zh^0} = M_Z^2/m_{h^0}^2$, $r_{ZH^0} = M_Z^2/m_{H^0}^2$, $r_{ZA^0} = M_Z^2/m_{A^0}^2$, $r_{ah^0} = M_{\chi_a^+}^2/m_{h^0}^2$, $r_{aH^0} = M_{\chi_a^+}^2/m_{H^0}^2$, $r_{aA^0} = M_{\chi_a^+}^2/m_{A^0}^2$, $r_{WH^+} = M_W^2/m_{H^+}^2$, $r_{aH^+} = M_{\chi_a^+}^2/m_{H^+}^2$, and $r_{iH^+} = M_{\chi_i^0}^2/m_{H^+}^2$, with $M_{W,Z}$, the masses of W and Z gauge bosons, m_{h^0, H^0, A^0, H^\pm} , the masses of Higgs bosons, and $M_{\chi_a^+} \geq 0$ and $M_{\chi_i^0} \geq 0$, the masses of charginos and neutralinos, respectively. The coefficients $c_{u,d,e}^{h^0, H^0, A^0, H^\pm}$ and matrices $D_{h^0, H^0}^{R,L}$, $G^{R,L}$, $E^{R,L}$, $M^{R,L}$, $N^{R,L}$ involve various combinations of the chargino and neutralino couplings to Higgs and gauge bosons, and are collected explicitly in the Appendix.

Before proceeding with our numerical study, we make several comments on the analytic results. First, we observe that the dependence on the CPV phases in the gauge-gaugino-Higgs-Higgsino sector is contained in the imaginary parts of the couplings $D_{S,aa}^R$, *etc.* but not separated out explicitly. As indicated in the Appendix, these phases arise from diagonalizing the chargino and neutralino mass matrices in Eq. (A3). In general, the resulting independent phases are $\text{Arg}(\mu M_i b^*)$ and $\text{Arg}(M_i M_j^*)$, where μ is the supersymmetric Higgs-Higgsino mass parameter; M_i ($i = 1, 2, 3$) are the soft gaugino mass parameters; and b is the soft Higgs mass parameter. The $\text{SU}(3)_C$ mass parameter does not enter the diagonalization of chargino-neutralino mass matrices, leaving two remaining phases. The analysis of CPV in this sector is often simplified by assuming that $\text{Arg}(M_1 M_2^*) = 0$, leaving one remaining, independent phase denoted ϕ_μ . In our numerical study below, we will adopt this simplifying assumption and verify numerically that each of the two-loop contributions is proportional to $\sin\phi_\mu$.

Second, we observe that the coefficients $c_f^{h^0}$ and $c_f^{H^0}$ given in Eq. (A1) as well as the matrices $D_{h^0}^{R,L}$ *etc.* given in Eq. (A2) depend in general on $\tan\beta = v_u/v_d$, where the v_k are the vacuum expectation values of the two neutral Higgs scalars, and Z_R , which further depends on m_{A^0} as illustrated in Eq. (A6). This introduces an additional dependence on

$\tan\beta$ and m_{A^0} beyond the explicit dependence generated by the Yukawa couplings and dependence of the loop functions on scalar masses.

Third, we observe that the overall sign of the WH^\pm contribution is opposite to that of the other contributions. The origin of this overall sign can be understood by considering the combinations of couplings and Lorentz structures entering the two loop amplitudes. To illustrate, we consider the loop of Fig. 1(a) that enters each of the contributions. To compare the relative signs of the couplings, we define a general set of interactions involving charginos, neutralinos, Higgs scalars, and fermions:

$$\begin{aligned}\mathcal{L}_{V\chi\chi} &= \bar{\chi}\gamma^\mu [A_L P_L + A_R P_R] \chi V_\mu + \dots \\ \mathcal{L}_{\phi\chi\chi} &= \bar{\chi} [B_L P_L + B_R P_R] \chi \phi + \dots \\ \mathcal{L}_{V\ell\ell} &= \bar{\ell}\gamma^\mu [C_L P_L + C_R P_R] \ell V_\mu + \dots \\ \mathcal{L}_{\phi\ell\ell} &= \bar{\ell} [D_L P_L + D_R P_R] \ell \phi + \dots\end{aligned}\tag{9}$$

In Table I below we give the corresponding phases of the couplings obtained from the Feynman rules of Ref. [16]. Now we consider the structure of the fermion line in the loop, which gives the only other source of a phase difference between the different contributions. If ℓ is the momentum flowing through the loop (we may neglect the external fermion momenta for this discussion), we have

$$\begin{aligned}ZA^0 &\sim \gamma^\mu [2T_3 P_L - 2Q \sin^2 \theta_W] \not{\ell} \gamma_5 \\ &= \gamma^\mu [-2T_3 P_L + 2Q \sin^2 \theta_W \gamma_5] \not{\ell} \\ &= \frac{1}{2} \gamma^\mu [-(2T_3 - 4Q \sin^2 \theta_W) \gamma_5 - 2T_3] \not{\ell} \\ Zh^0 &\sim \gamma^\mu [2T_3 P_L - 2Q \sin^2 \theta_W] \not{\ell} \\ &= \frac{1}{2} \gamma^\mu [(2T_3 - 4Q \sin^2 \theta_W) - 2T_3 \gamma_5] \not{\ell} \\ WH^\pm &\sim \gamma^\mu P_L \not{\ell} P_R = \gamma^\mu P_L \not{\ell} = \frac{1}{2} \gamma^\mu (1 - \gamma_5) \not{\ell}\end{aligned}\tag{10}$$

For the case of ZA^0 exchange which involves $T^{\mu\nu}$ from the closed chargino loop, we require the γ_5 term from the lower line to obtain the EDM, whereas for Zh^0 exchange, we have the pseudo-tensor $P^{\mu\nu}$ from the closed chargino loop, necessitating that we retain the identity matrix term from the fermion line. For the WH^\pm exchange contribution, we require both. Table II gives the resulting overall phase for the various contributions.

TABLE I: Phases of couplings in Eq. (9) as they enter the amplitude of Fig. 1(a)

Vertex	ZA	Zh^0	WH^\pm
$V\chi\chi$	$-i$	$-i$	$+i$
$\phi\chi\chi$	$+1$	$-i$	$+i$
$\phi\ell\ell$	$+1$	$+i$	$-i$
$V\ell\ell$	$+i$	$+i$	$+i$
Overall	$+1$	$+1$	-1

We observe that the part of the WH^\pm exchange graph arising from the $T^{\mu\nu}$ tensor should have an opposite, overall phase compared to the corresponding ZA exchange diagram. Similarly, the $P^{\mu\nu}$ component of the WH^\pm loop and the Zh^0 graph will also differ in overall relative phase. Note that there is an additional overall phase that arises between the $T^{\mu\nu}$ and $P^{\mu\nu}$ terms when the identity

$$\varepsilon^{\mu\nu\alpha\beta}\sigma_{\alpha\beta} = -2i\sigma^{\mu\nu}\gamma_5$$

is used in the terms generated by $P^{\mu\nu}$. Thus, the relative sign between the ZA^0 and Zh^0 graphs are the same, as are the relative phase between the $T^{\mu\nu}$ and $P^{\mu\nu}$ terms in the WH^\pm contribution.

Fourth, we note that our results for the γh^0 , γA^0 , and Zh^0 amplitudes agree with those of Ref. [9, 10, 11], including the overall phase. On the surface, our result for the Zh^0 contribution appears to be different from the expression given in Ref. [11]. The difference amounts to replacing the x^{-1} in Eq. (5) by $[2x(1-x)]^{-1}$ to convert the integral to that of Ref. [11]. However, after taking into account the symmetry properties of the integrands in both expressions, we have verified (both analytically and numerically) that they agree.

Finally, we note that a direct comparison of our analytic results with those obtained in Ref. [14] is not straightforward, since the latter employed an effective field theory approach. We note, however, that these authors also include a nonzero result for the ZZ -exchange contribution that the authors of Ref. [11] argued should vanish. A direct comparison of numerical results is also challenging, since only the dependence of the EDMs on the CPV phases was given in Ref. [14], whereas in our numerical study below, we explore the dependence on mass parameters and $\tan\beta$ for fixed values of ϕ_μ .

III. NUMERICAL ANALYSIS

In this section we numerically assess the impact of the additional, two-loop EDM contributions discussed above. As mentioned in the Introduction, one motivation for our work to consider the complete set of two-loop Higgs-mediated chargino-neutralino contributions stems from the framework of EWB. It is therefore natural and well-motivated to focus a portion of our numerical analysis on a supersymmetric setup which is compatible with that framework. Before doing so, however, we investigate the relative importance of the various contributions and their dependence on MSSM parameters.

To that end, we define a benchmark parameter set scenario that will serve as a basis for comparison, motivated by the EWB framework, and consistent with phenomenological and cosmological constraints, as discussed below. We then proceed with a scan over pairs

TABLE II: Summary of signs from fermion line and overall result. The final row is obtained by multiplying the overall phases from Table I and the sign obtained from the fermion line.

Graph	ZA ($T^{\mu\nu}$)	Zh^0 ($P^{\mu\nu}$)	WH^\pm ($T^{\mu\nu}$)	WH^\pm ($P^{\mu\nu}$)
γ -matrix	γ_5	1	γ_5	1
sign	-1	+1	-1	+1
Overall	-1	+1	+1	-1

of parameters that govern the size of EDMs, keeping the other parameters fixed at their benchmark values. To suppress one-loop EDM contributions, we assume all sfermions to be decoupled (we set all sfermion soft breaking masses to 10 TeV, and the trilinear scalar couplings to zero, for definiteness). The gluino mass is entirely unimportant for the phenomenology discussed here, and is set to 1 TeV. The remaining parameters relevant for the two-loop EDM contributions are the absolute values of the gaugino soft breaking masses $M_{1,2}$ and of the higgsino mass parameter μ , the heavy MSSM Higgs mass scale (for definiteness we employ here as a free parameter m_{A^0}), and $\tan\beta$. Our reference benchmark setup is! defined as follows:

$$M_1 = 145 \text{ GeV}, \quad M_2 = 290 \text{ GeV}, \quad \mu = 300 \text{ GeV}, \quad m_{A^0} = 300 \text{ GeV}, \quad \tan\beta = 10. \quad (11)$$

We consider here one single CP-violating phase, ϕ_μ , as discussed above. We set this phase $\phi_\mu = \pi/2$, giving the largest CP-violating effect. We verified numerically that the EDMs considered here scale proportionally to $\sin\phi_\mu$ to within an accuracy of 1%. This means that (1) all the results we show below can be simply re-scaled when assuming a non-maximal CP-violating phase and (2) we show the largest possible size for the EDM contributions we consider here³. Notice that the values for m_{h^0} and α are obtained numerically at two-loop order through the FeynHiggs package [18].

We have chosen this particular benchmark setup for several reasons. First, this choice is potentially compatible with successful EWB. Second, the lightest neutralino relic abundance is close to the observed cold dark matter density [19]. If the relic neutralino abundance were larger than the cold dark matter density, a mechanism would be needed to dilute the relic abundance, with implications for EWB as well [20]. Third, the parameter values given above are consistent with collider searches, with precision electroweak data, including the muon anomalous magnetic moment, and with the inclusive branching ratio $b \rightarrow s\gamma$ [21]. The latter constraint is particularly critical at low m_{A^0} , since contributions to $b \rightarrow s\gamma$ from the top-quark- H^\pm loop can be sizable.

Starting from this reference point, we first illustrate the relative magnitude of two-loop contributions in Fig. 2. Here, we explore these contributions to the EDM of the electron (left panel) and the neutron (right panel) as a function of $\tan\beta$, with all other parameters set as in Eq. (11). To illustrate our results on a logarithmic scale, we show absolute values and indicate with black lines positive contributions and with red lines negative ones. Notice that we do include the WW contribution in our numerical analysis, taking the expression for this contribution from Ref. [11].

The curves in Fig. 2 lead to several observations.

- (i) We notice that for both the WW and the WH^\pm contributions a cancellation among the couplings that yield the overall coefficients of these terms occurs at low $\tan\beta$. The resulting suppression of these contributions in this region is due to the particular values of the $M_{1,2}$ and μ parameters we picked and the fact that the various chargino-neutralino contributions over which we sum enter with different relative signs.
- (ii) The only contribution that appears to scale clearly and rapidly with $\tan\beta$ is the WH^\pm contribution. While other contributions have explicit, overall $\tan\beta$ factors, the relevant neutralino and chargino couplings conspire to induce, a net $1/\tan\beta$ contribution. We numerically verified this scaling, *e.g.*, for the γA^0 and ZA^0 contributions.

³ We remind the reader that EWB implies $\sin\phi_\mu \gtrsim 10^{-2}$ [17].

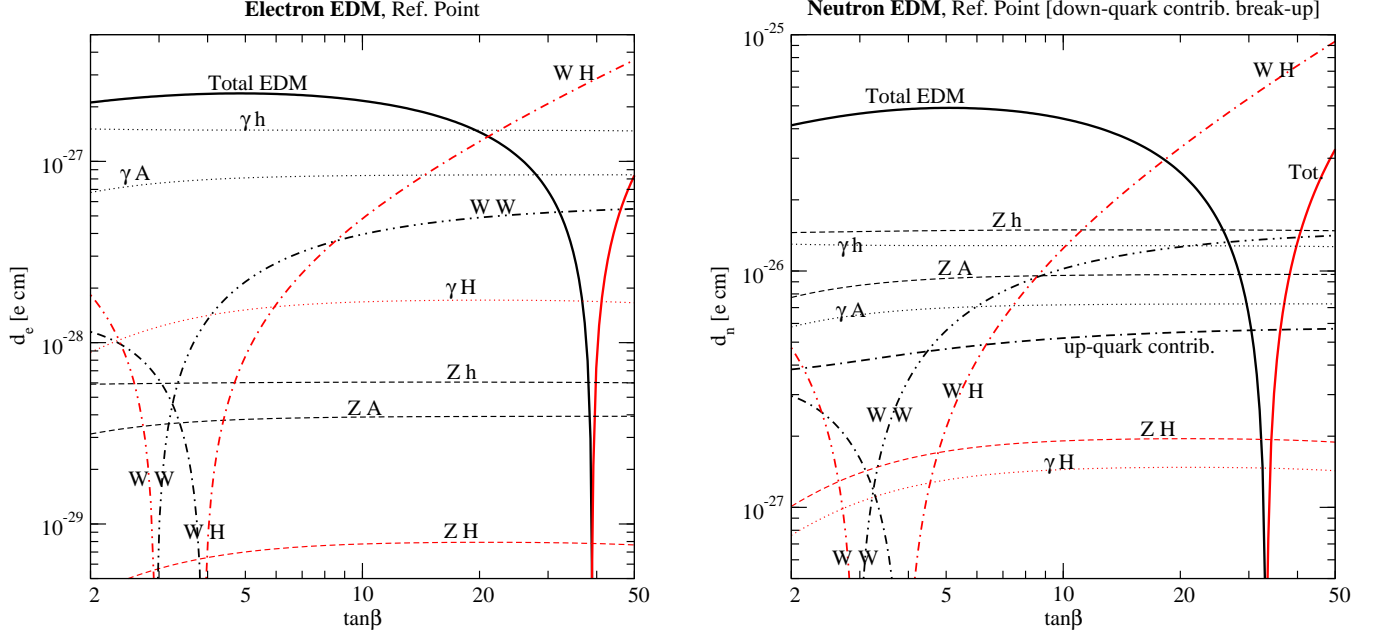


FIG. 2: A break-up of the various Higgs-mediated chargino-neutralino two-loop contributions to the electron (left) and neutron (right) electric dipole moment. Black lines correspond to positive values, red lines to negative values. In the right panel we show the various down-quark contributions times a factor $4/3$, as well as the global up-quark contribution (times a factor $-1/3$). All SUSY parameters, except $\tan\beta$, are fixed to the reference setup.

- (iii) The dominant contributions to the electron EDM appear to be the γh^0 and the γA^0 loops. However notice that the WH^\pm contribution dominates at large $\tan\beta$, and that the WW contribution is also sizable, outside the region where the suppression of its overall coefficient occurs. The Z plus Higgs contributions are suppressed by the $T_{3e_L} - 2s_W^2 Q_e$ factor, and are subdominant. In general, contributions involving the heavy CP-even Higgs H^0 are suppressed relative to both those involving h^0 and A^0 .
- (iv) The dominant contributions at low $\tan\beta$ are eventually canceled out by the growing and negative WH^\pm contribution as $\tan\beta$ is increased. For the electron EDM, the cancellation of the various two-loop contributions is driven by the opposite signs of the γh^0 and γA^0 contributions compared to that from the WH^\pm loops.
- (v) A similar picture applies to the case of the neutron EDM. Here we explicitly show only the break-up for the down-quark EDM (times a factor $4/3$), and the overall up-quark contribution (times a factor $1/3$: the contribution itself is thus always negative). As opposed to the electron EDM, the Z loops with h^0 and A^0 dominate the down-quark EDM, and the overall $d_n = 0$ effect is driven by the opposite signs of these contributions (and to a lesser extent the $\gamma h^0, A^0$ loops) compared to that of the WH^\pm one.

Using the foregoing considerations, we now study the dependence of the total two-loop EDMs as a function of various MSSM parameters. First, we investigate the $(\tan\beta, m_{A^0})$ sector. This sets the mass scale for all loops involving H^0, A^0 and H^\pm , as well as various couplings, directly [see e.g. Eq. (A1)] or indirectly, *e.g.*, through electroweak symmetry

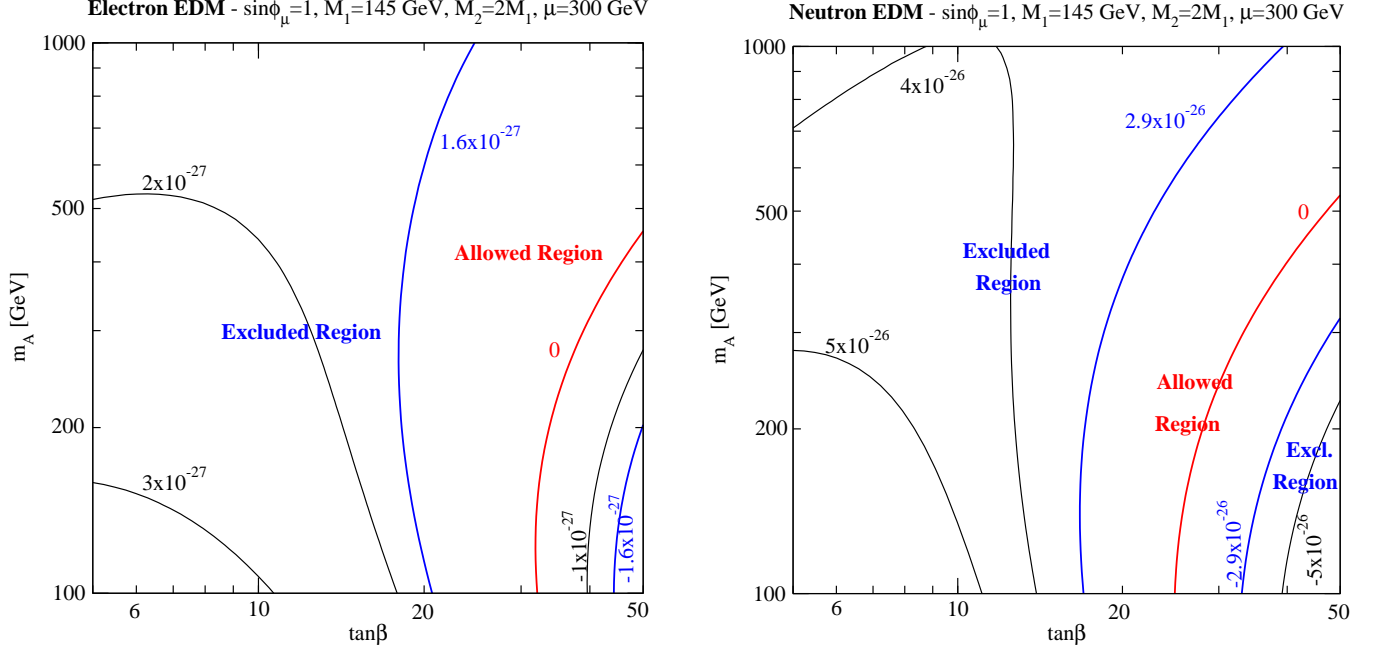


FIG. 3: Contours of constant electron (left) and neutron (right) electric dipole moment, on the $(\tan\beta, m_{A^0})$ plane, for $M_1 = 145$ GeV, $M_2 = 290$ GeV, $\mu = 300$ GeV and $\sin\phi_\mu = 1$. For this particular point in parameter space, the allowed region lies between the blue lines. The locus where the 2-loop contributions under investigation here cancel out is indicated by the red line.

breaking effects in the neutralino and chargino mass and mixing matrices. We explore the EDM dependence on $(\tan\beta, m_{A^0})$ in Fig. 3, setting again all other supersymmetric parameters to the values indicated in (11). In the low $\tan\beta$ region we do find – as expected – a suppression of the EDM with increasing m_{A^0} at fixed values of $\tan\beta$. The most striking feature of this parameter analysis, however, is the existence of a line of points where the sum of the two-loop contributions adds up to zero (red line). For the particular values of the supersymmetric parameters chosen here, the allowed region lies in the relatively narrow strip at $20 \lesssim \tan\beta \lesssim 50$. The main driver of the pattern we find is the cancellation among the various two-loop contributions discussed above. As for the difference between the electron and the neutron EDM, we point out that the allowed regions and the location of the two-loop cancellation line are rather similar. Presumably, this similarity indicates that (1) the up-quark contribution to d_n is subdominant (see Fig. 2, right panel) and that (2) there are a few dominant contributions to d_e and to d_d that are simply proportional to each other, and hence that cancel for the same parameter values. However, we do find that the scaling of d_n with m_{A^0} appears steeper than for d_e . In either case, the existence of the regions where the EDMs becomes nearly vanishing suggest that null results for future d_e and d_n searches could still be consistent with an $\mathcal{O}(1)$ phase ϕ_μ and electro weak scale masses in the gaugino-gauge-Higgsino-Higgs sector of the MSSM. This feature of the full two-loop computation was not identified in Ref. [14].

To make the connection with EWB, we now analyze the $(\mu, M_{1,2})$ -dependence of the two-loop EDMs. A generic expectation of the EWB scenario for the MSSM particle spectrum includes a relatively light mass scale for the heavy MSSM Higgs sector. This scenario depends on the suppression of the net baryon number density generated at the EW phase

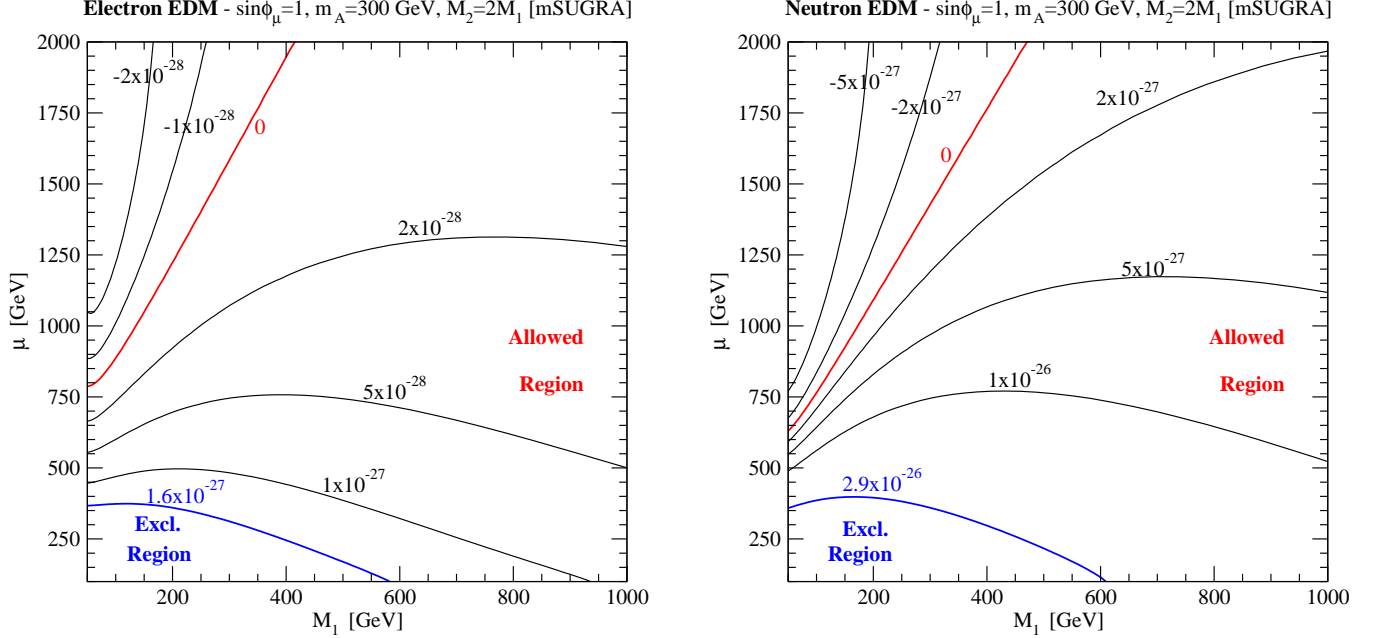


FIG. 4: Contours of constant electron (left) and neutron (right) electric dipole moment, on the (M_1, μ) plane. We assume the gaugino unification mass relation $M_2 \simeq 2M_1$, and assume maximal CP violation, $\sin \phi_\mu = 1$ (see the text for further details on the model assumptions). The bottom left regions (blue boundary) are experimentally ruled out.

transition with m_{A^0} , as pointed out and quantified *e.g.* in Ref. [22]. It was also realized in several analyses (see *e.g.* Ref. [17, 20, 23] and references therein), that the requirement of sufficiently large CP-violating sources for successful EWB prefers a resonant enhancement in the higgsino-gaugino sources. This resonance occurs for $M_1 \sim \mu$, the resonant neutralino baryogenesis funnel, or $M_2 \sim \mu$, the resonant chargino baryogenesis funnel, with $M_{1,2}, \mu \lesssim 1$ TeV. An additional resonance could occur for the CPV stop sources, but the latter possibility is generally precluded by the LEP limits on the mass of the h^0 . In both cases, however, successful EWB implies sub-TeV masses for higgsinos and gauginos.

Another generic feature of the MSSM spectrum implied by successful EWB is a light, mostly right-handed stop, in order to make the EW phase transition more strongly first order. Several studies pointed out, however, that an extended, non-minimal Higgs sector can also significantly (and perhaps more naturally) enhance the first-order character of the EW phase transition [24, 25]. We thus do not regard the requirement of a light stop as a necessary feature of a supersymmetric setup giving successful EWB. From the viewpoint of EDMs, we considered and evaluated the size of the two-loop stop-mediated contributions in [17], and concluded that they are subdominant, provided the left-handed stop is heavy enough, as required for EWB in the MSSM⁴. In the interest of singling out the two-loop Higgs-mediated chargino-neutralino contributions under investigation here, and in view of the above considerations, we do not assume a light right handed stop.

Having these considerations in mind, we illustrate in Fig. 4 the values of the electron (left) and of the neutron (right) EDM in the (M_1, μ) plane. We assume a minimal supergravity-

⁴ Note that this requirement stems primarily from having a Higgs mass consistent with the LEP limits

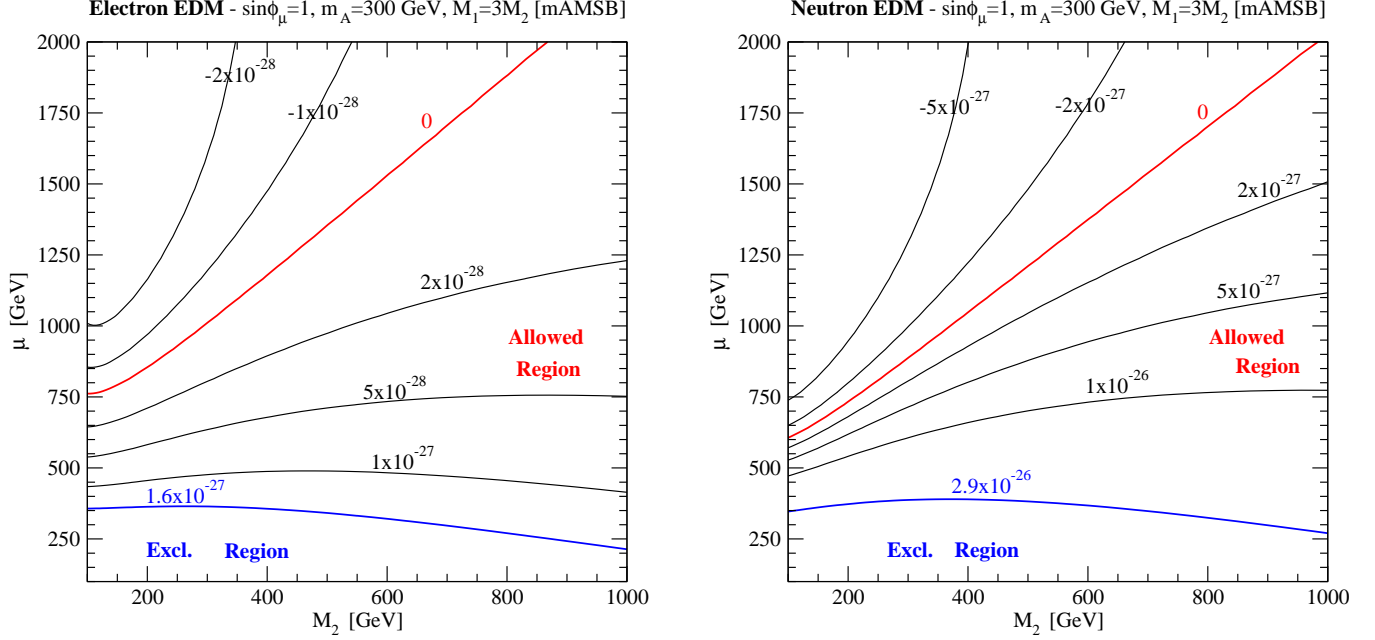


FIG. 5: Contours of constant electron (left) and neutron (right) electric dipole moment, on the (M_2, μ) plane. We assume here the anomaly-mediated SUSY breaking gaugino mass relation $M_1 \simeq 3M_2$, and assume maximal CP violation, $\sin \phi_\mu = 1$ (see the text for further details on the model assumptions). The bottom regions (below the blue boundary) are experimentally ruled out.

type relation⁵ between the gaugino soft breaking masses (where gaugino masses unify at the GUT scale, and their EW-scale values are set by renormalization group running), and set here $M_2 = 2M_1$. In addition, $\tan \beta$ and m_{A^0} are set to the reference values listed in Eq. (11). Both EDMs are positive in the lower-right portion of the plot, and negative in the upper-left corner (low M_1 and large μ). A line exists, for both the electron and the neutron EDM, where the two-loop contributions under consideration here exactly cancel out. We indicate this line in red, and label it with a zero. In the low μ and low M_1 region the size of the two-loop contribution exceeds the experimentally viable values (which we take to be $d_e < 1.6 \times 10^{-27}$ e cm and $d_n < 2.9 \times 10^{-26}$ e cm). We indicate the boundaries of the excluded region with blue lines. The parameter space above the blue lines is currently experimentally open.

Depending on the supersymmetry breaking mechanism, gaugino masses can be related by different functional forms. For instance, if supersymmetry breaking is dominated by anomaly mediation, then one expects $M_1 \simeq 3M_2$, hence an inverted bino-wino hierarchy with respect to a gaugino-unified setup (see e.g. [26]). We study this possibility in Fig. 5, where we explore the values of the electron (left) and neutron (right) EDM on the (M_2, μ) plane, setting $M_1 = 3M_2$ and the other parameters as in the benchmark model. We observe a pattern for the EDM very much similar to the one obtained for the gaugino-unification type scenario: the parameter space is split into a negative and a positive EDM region, and there

⁵ Notice that the label “[mSUGRA]” obviously doesn’t refer to the usual minimal supergravity setup, but only to the gaugino mass relation being employed here. The same applies to the label “[mAMSB]” of fig. 5.

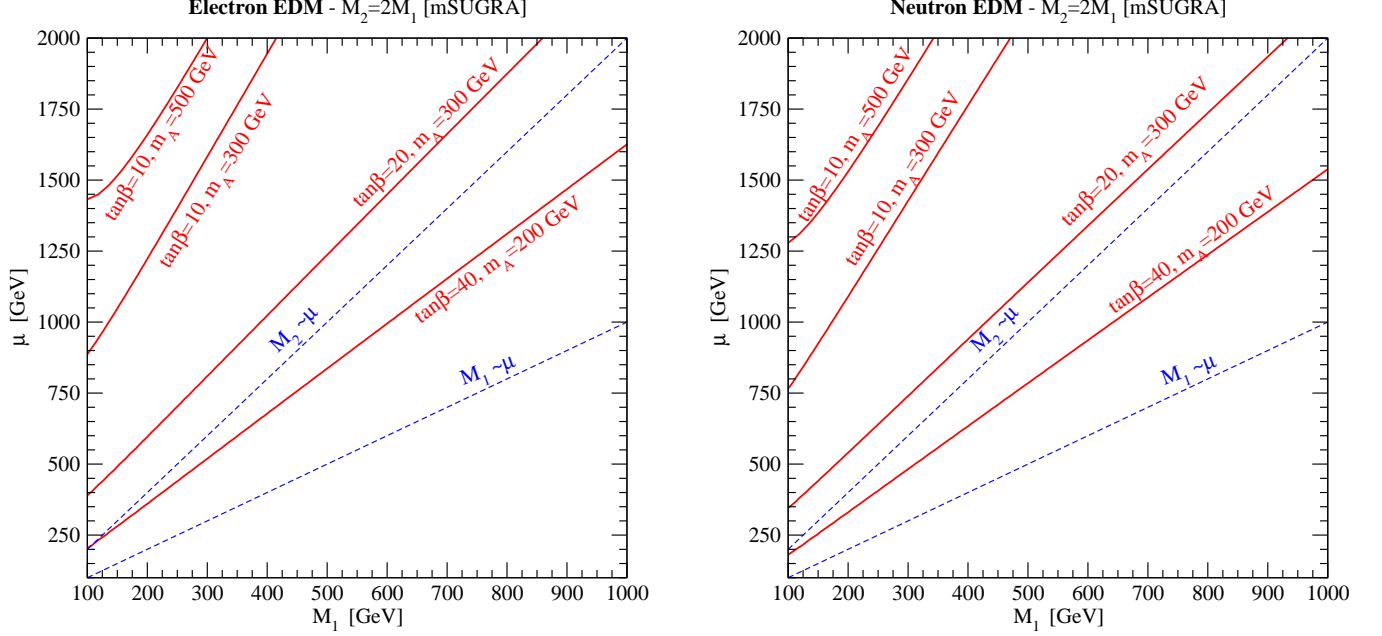


FIG. 6: The location of the exact cancellation in the 2-loop contributions under consideration here on the (M_1, μ) plane, for given $\tan \beta$ and m_{A^0} . The left panel shows the points where $d_e = 0$, while the right panel indicates where $d_n = 0$. We assume here that $M_2 = 2M_1$

exist parameter space points where the two-loop contributions vanish. As in Fig. 4, the region at small μ produces, for maximal CP-violating phases, values for the EDM in excess of the current experimental constraints. We comment below on the location of the “cancellation line” (giving zero two-loop EDM) its dependence on the various model parameters.

The specific location of the cancellation lines depends upon the particular values of the model parameters used. Assuming $M_2 = 2M_1$, we show in Fig. 6 where the cancellation takes place for the electron (left) and neutron (right) EDM in the (M_1, μ) plane, for given $\tan \beta$ and m_{A^0} . We also indicate, with dashed blue lines, the $M_1 = \mu$ and $M_2 = \mu$ lines, where resonant neutralino and chargino driven EWB is more effective (see below). First, we notice that the cancellations occur along straight lines, when $M_{1,2}, \mu \gg m_Z$ (i.e. outside the region where electro-weak mixing is relevant). This fact is simply understood by noticing that the EDM’s can be approximately re-expressed as functions of gaugino and higgsino mass *ratios*, e.g. $r_\mu = \mu/M_2$, $r_1 = M_1/M_2$ etc. The location of the cancellation is close to a scale-free problem, i.e., it does not depend upon the overall mass-scale (in our example, M_2). Therefore, if $d(\mu^0, M_1^0, M_2^0) = 0$ then we expect $d(\mu^1, M_1^1, M_2^1) \simeq 0$, where $\mu^0 = \alpha\mu^1$, and α is a real number.

Turning now to the specific location of the cancellation as a function of the values assumed for $\tan \beta$ and m_{A^0} , we find that the smaller $\tan \beta$, the larger μ needs to be for a given M_1 . The slope of the cancellation line appears to be a function of $\tan \beta$, and it steepened at lower value of $\tan \beta$. By comparison, m_{A^0} sets the scale for μ where the cancellation takes place, at given M_1 . Again, we observe very similar patterns for the electron and for the neutron EDM. Interestingly, we find that the cancellation of two-loop contributions for low values of $\tan \beta$, generally favored in minimal EWB setups [22], occurs outside the region of resonant EWB. In particular, we do not find any phenomenologically viable combination of $(\tan \beta, m_{A^0})$ that brings the cancellation down to the resonant neutralino-driven line $M_1 \sim \mu$. Neutralino-

driven EWB seems thus to be “protected” against vanishing two-loop EDM contributions. Of course, cancellations between the one and two-loop contribution might still be possible [20].

In summary, our numerical results indicate that the WH^\pm contribution computed here is the dominant EDM two-loop contribution in the large $\tan\beta$ regime (in the limit of heavy sfermions). The WH^\pm diagram negatively interferes with the dominant γh^0 , γA^0 (for the electron EDM) and Zh^0 , ZA^0 (for the neutron EDM) contributions, yielding a cancellation in the overall two-loop EDM.

IV. SUMMARY AND CONCLUSIONS

The analysis we have completed gives the EDMs of the electron and neutron in the MSSM when the sfermion masses are large, leading to a suppression of the one-loop contributions and general dominance of two-loop terms. Considering this regime allows one to circumvent the SUSY CP problem associated with the present, stringent EDM limits and sub-TeV scale sfermions. It also implies vanishing EDMs for diatomic atoms, assuming they are generated primarily by the chromo-EDMs of the quarks⁶. Previous studies of this regime have generally also taken all but the lightest, SM-like CP-even scalar to be heavy, thereby suppressing two-loop contributions involving the other Higgs scalars as well. In the present study, we have not made these assumptions and have, instead, analyzed the dependence of the two-loop EDMs on the full gauge-gaugino-Higgs-Higgsino parameter space of the MSSM.

Our primary results are that (a) contributions arising from exchanges involving one SM gauge boson and either the CP-odd neutral scalar, A^0 , or the charged Higgs scalars, H^\pm , can be comparable to previously considered contributions, and (b) for sufficiently large $\tan\beta$, strong cancellations may occur between the WH^\pm exchange diagrams and those involving neutral bosons. These cancellations can lead to a vanishing EDM of the electron and neutron if m_{A^0} is in the non-decoupling regime. This second result implies that if future electron and neutron EDM searches – with sensitivities enhanced by factors of 10 to 100 – obtain null results, SUSY CPV with order one phases and electroweak scale charginos, neutralinos, and Higgs scalars may not be excluded. We have also analyzed the prospective implications for MSSM electroweak baryogenesis, whose viability depends in part on the values of $\tan\beta$ and m_{A^0} . Although a definitive conclusion awaits a future, more comprehensive study [20], our analysis here suggests that if MSSM EWB is driven by the precursors of neutralinos, then the aforementioned cancellations would not take place and that future EDM searches could expect to yield a non-zero result.

Acknowledgements

We thank G. Giudice and A. Romanino for helpful discussions regarding the results for the Zh^0 contributions. This work was supported in part under U.S. Department of Energy Contracts DE-FG02-08ER41531(YL and MJRM) and the University of Wisconsin Alumni Research Foundation (YL and MJRM), and by a Faculty Research Grant from the University of California, Santa Cruz (SP).

⁶ See Ref. [4] for a detailed discussion of the effective operator-dependence of various EDMs.

APPENDIX A: COEFFICIENTS, MATRICES, AND LOOP FUNCTION

The coefficients $c_{u,d,e}^{h^0, H^0, A^0, H^+}$ depend on specific types of Higgs bosons and SM fermions

$$\begin{aligned} c_u^{h^0} &= \frac{Z_R^{21}}{\sin\beta}, \quad c_d^{h^0} = c_e^{h^0} = \frac{Z_R^{11}}{\cos\beta}, \quad c_u^{H^0} = \frac{Z_R^{22}}{\sin\beta}, \quad c_d^{H^0} = c_e^{H^0} = \frac{Z_R^{12}}{\cos\beta}, \\ c_u^{A^0} &= \cot\beta, \quad c_d^{A^0} = c_e^{A^0} = \tan\beta, \quad c_u^{H^+} = \cot\beta, \quad c_d^{H^+} = c_e^{H^+} = \tan\beta. \end{aligned} \quad (\text{A1})$$

The matrices $D_{h^0, H^0}^{R,L}, G^{R,L}, E^{R,L}, M^{R,L}, N^{R,L}$ are

$$\begin{aligned} D_{h^0, ab}^R &= Z_R^{11} Z_-^{2b*} Z_+^{1a*} + Z_R^{21} Z_-^{1b*} Z_+^{2a*}, \\ D_{h^0, ab}^L &= Z_R^{11} Z_-^{2a} Z_+^{1b} + Z_R^{21} Z_-^{1a} Z_+^{2b}, \\ D_{H^0, ab}^R &= Z_R^{12} Z_-^{2b*} Z_+^{1a*} + Z_R^{22} Z_-^{1b*} Z_+^{2a*}, \\ D_{H^0, ab}^L &= Z_R^{12} Z_-^{2a} Z_+^{1b} + Z_R^{22} Z_-^{1a} Z_+^{2b}, \\ G_{ab}^R &= \frac{1}{2}(Z_-^{1a} Z_-^{1b*} + \delta^{ab}(c_W^2 - s_W^2)), \\ G_{ab}^L &= \frac{1}{2}(Z_+^{1a*} Z_+^{1b} + \delta^{ab}(c_W^2 - s_W^2)), \\ E_{ab}^R &= \sin\beta Z_-^{2b*} Z_+^{1a*} + \cos\beta Z_-^{1b*} Z_+^{2a*}, \\ E_{ab}^L &= -(\sin\beta Z_-^{2a} Z_+^{1b} + \cos\beta Z_-^{1a} Z_+^{2b}), \\ M_{ai}^R &= Z_-^{1a} Z_N^{2i*} + \frac{1}{\sqrt{2}} Z_-^{2a} Z_N^{3i*}, \\ M_{ai}^L &= Z_+^{1a*} Z_N^{2i} - \frac{1}{\sqrt{2}} Z_+^{2a*} Z_N^{4i}, \\ N_{ai}^R &= -\cos\beta \left(\frac{1}{\sqrt{2}} Z_+^{2a*} (Z_N^{1i*} s_W + Z_N^{2i*} c_W) + Z_+^{1a*} Z_N^{4i*} c_W \right), \\ N_{ai}^L &= \sin\beta \left(\frac{1}{\sqrt{2}} Z_-^{2a} (Z_N^{1i} s_W + Z_N^{2i} c_W) - Z_-^{1a} Z_N^{3i} c_W \right), \end{aligned} \quad (\text{A2})$$

with $\tan\beta = v_u/v_d$.

The $Z_{\pm, N}$ are diagonalization matrices of chargino and neutralino mass matrices $Z_-^T M_C Z_+ = \text{Diag}(M_{\chi_1^+}, M_{\chi_2^+})$, $Z_N^T M_N Z_N = \text{Diag}(M_{\chi_1^0}, M_{\chi_2^0}, M_{\chi_3^0}, M_{\chi_4^0})$, with $M_{\chi_a^+} > 0$, $M_{\chi_i^0} > 0$, and

$$\begin{aligned} M_C &= \begin{pmatrix} M_2 & \sqrt{2} M_W \cos\beta \\ \sqrt{2} M_W \sin\beta & \mu \end{pmatrix}, \\ M_N &= \begin{pmatrix} M_1 & 0 & -M_Z s_W \cos\beta & M_Z s_W \sin\beta \\ 0 & M_2 & M_Z c_W \cos\beta & -M_Z c_W \sin\beta \\ -M_Z s_W \cos\beta & M_Z c_W \cos\beta & 0 & -\mu \\ M_Z s_W \sin\beta & -M_Z c_W \cos\beta & -\mu & 0 \end{pmatrix}. \end{aligned} \quad (\text{A3})$$

The Z_R in c^{h^0, H^0} and $D_{h^0, H^0}^{R,L}$ is the matrix that diagonalize the mass matrix of CP-even neutral Higgs bosons

$$\sqrt{2} \begin{pmatrix} \text{Re}[H_d^0] - v_d \\ \text{Re}[H_u^0] - v_u \end{pmatrix} = Z_R \begin{pmatrix} h^0 \\ H^0 \end{pmatrix}, \quad (\text{A4})$$

which, expressed in terms of α , takes the form

$$Z_R = \begin{pmatrix} -\sin\alpha & \cos\alpha \\ \cos\alpha & \sin\alpha \end{pmatrix}. \quad (\text{A5})$$

The α , at tree level, can be expressed as

$$\tan\alpha = \frac{-(M_{A^0}^2 - M_Z^2)\cos 2\beta - \sqrt{(M_{A^0}^2 + M_Z^2)^2 - 4M_{A^0}^2 M_Z^2 \cos^2 2\beta}}{(M_{A^0}^2 + M_Z^2)\sin 2\beta}. \quad (\text{A6})$$

Notice that α is approximately $\beta - \pi/2$ at the limit $M_{A^0} \gg M_Z$. Radiative corrections modify the latter relation, and we include these effects in our numerical study.

The loop function $j(r, r')$ is the same as in Ref. [11]

$$j(r) = \frac{r \text{Log} r}{r - 1}, \quad j(r, r') = \frac{j(r) - j(r')}{r - r'}. \quad (\text{A7})$$

-
- [1] B. C. Regan, E. D. Commins, C. J. Schmidt and D. DeMille, *Phys. Rev. Lett.* **88** (2002) 071805
 - [2] C. A. Baker. *et al.*, arXiv:hep-ex/0602020 (2006)
 - [3] M. V. Romalis, W. C. Griffith and E. N. Fortson, *Phys. Rev. Lett.* **86** (2001) 2505
 - [4] M. Pospelov and A. Ritz, *Annals Phys.* **318**, 119 (2005) [arXiv:hep-ph/0504231].
 - [5] M. J. Ramsey-Musolf and S. Su, *Phys. Rept.* **456**, 1 (2008) [arXiv:hep-ph/0612057].
 - [6] A. G. Cohen, D. B. Kaplan and A. E. Nelson, *Phys. Lett. B* **388**, 588 (1996) [arXiv:hep-ph/9607394].
 - [7] D. Chang, W. Y. Keung and A. Pilaftsis, *Phys. Rev. Lett.* **82**, 900 (1999) [Erratum-ibid. **83**, 3972 (1999)] [arXiv:hep-ph/9811202], A. Pilaftsis, *Phys. Lett. B* **471**, 174 (1999) [arXiv:hep-ph/9909485].
 - [8] D. Chang, W. F. Chang and W. Y. Keung, *Phys. Lett. B* **478**, 239 (2000) [arXiv:hep-ph/9910465].
 - [9] D. Chang, W. F. Chang and W. Y. Keung, *Phys. Rev. D* **66**, 116008 (2002) [arXiv:hep-ph/0205084].
 - [10] A. Pilaftsis, *Nucl. Phys. B* **644**, 263 (2002) [arXiv:hep-ph/0207277].
 - [11] G. F. Giudice and A. Romanino, *Phys. Lett. B* **634**, 307 (2006) [arXiv:hep-ph/0510197].
 - [12] D. Chang, W. F. Chang and W. Y. Keung, *Phys. Rev. D* **71**, 076006 (2005) [arXiv:hep-ph/0503055].
 - [13] S. M. Barr and A. Zee, *Phys. Rev. Lett.* **65**, 21 (1990) [Erratum-ibid. **65**, 2920 (1990)].
 - [14] T. F. Feng, L. Sun and X. Y. Yang, arXiv:0805.1122 [hep-ph].
 - [15] K. Fujikawa, *Phys. Rev. D* **7** (1973) 393, M. B. Gavela, G. Girardi, C. Malleville and P. Sorba, *Nucl. Phys. B* **193**, 257 (1981), J. C. Romao and A. Barroso, *Phys. Rev. D* **35**, 2836 (1987).
 - [16] J. Rosiek, arXiv:hep-ph/9511250.
 - [17] V. Cirigliano, S. Profumo and M. J. Ramsey-Musolf, *JHEP* **0607**, 002 (2006) [arXiv:hep-ph/0603246].
 - [18] S. Heinemeyer, W. Hollik and G. Weiglein, *Comput. Phys. Commun.* **124** (2000) 76 [arXiv:hep-ph/9812320].

- [19] E. Komatsu *et al.* [WMAP Collaboration], arXiv:0803.0547 [astro-ph].
- [20] V. Cirigliano, Y. C. Li, S. Profumo and M. J. Ramsey-Musolf, in preparation.
- [21] W. M. Yao *et al.* [Particle Data Group], J. Phys. G **33**, 1 (2006).
- [22] J. M. Moreno, M. Quiros and M. Seco, Nucl. Phys. B **526** (1998) 489 [arXiv:hep-ph/9801272].
- [23] M. S. Carena, M. Quiros, M. Seco and C. E. M. Wagner, Nucl. Phys. B **650**, 24 (2003) [arXiv:hep-ph/0208043].
- [24] M. Pietroni, Nucl. Phys. B **402** (1993) 27 [arXiv:hep-ph/9207227], A. T. Davies, C. D. Froggatt and R. G. Moorhouse, Phys. Lett. B **372** (1996) 88 [arXiv:hep-ph/9603388], S. J. Huber and M. G. Schmidt, Nucl. Phys. B **606** (2001) 183 [arXiv:hep-ph/0003122], M. Bastero-Gil, C. Hugonie, S. F. King, D. P. Roy and S. Vempati, Phys. Lett. B **489**, 359 (2000) [arXiv:hep-ph/0006198], J. Kang, P. Langacker, T. j. Li and T. Liu, Phys. Rev. Lett. **94**, 061801 (2005) [arXiv:hep-ph/0402086], A. Menon, D. E. Morrissey and C. E. M. Wagner, Phys. Rev. D **70**, 035005 (2004) [arXiv:hep-ph/0404184], C. Grojean, G. Servant and J. D. Wells, Phys. Rev. D **71**, 036001 (2005) [arXiv:hep-ph/0407019], M. Carena, A. Megevand, M. Quiros and C. E. M. Wagner, Nucl. Phys. B **716**, 319 (2005) [arXiv:hep-ph/0410352].
- [25] S. Profumo, M. J. Ramsey-Musolf and G. Shaughnessy, JHEP **0708** (2007) 010 [arXiv:0705.2425 [hep-ph]].
- [26] T. Moroi and L. Randall, Nucl. Phys. B **570**, 455 (2000) [arXiv:hep-ph/9906527].